ChemComm

Stackable Molecular Chairs

Journal:	*ChemComm*
Manuscript ID	CC-COM-02-2019-001664.R2
Article Type:	Communication

COMMUNICATION

Stackable Molecular Chairs

Rezceived 00th January 20xx,
Accepted 00th January 20xx

DOI: 10.1039/x0xx00000x

Han Xie, Lei Zhiquan, Radoslav Z. Pavlović, Judith Gallucci and Jovica D. Badjić*

We describe design, preparation and assembly of chair-shaped molecules, comprising a *tris*-bicyclo[2.2.1]heptane hub that extends into three phthalimides carrying amino acids or short peptides. In water, molecular chairs stack in antiparallel manner to give hexavalent dendritic structures, in spite of holding equal charges. Here described strategy for increasing multivalency of peptides is easy to implement in practice therefore holding a potential for creating novel soft materials and therapeutics.

The assembly of stable and hierarchical soft materials[1] is, in water,[2] often a balancing act between hydrophobic effect[3] and ionic interactions.[4] Amphiphilic or bolaamphiphilic molecules, with non-polar and charged domains, could thus pack[5] into membranes, tubes, micelles or vesicles in spite of their ionic groups holding the same type of charge and being juxtaposed to one another.[6] For non-covalent host-guest complexes, however, the formation of stable structures would in most cases necessitate for charged domains to be attractive;[7] In the face of such conventional wisdom,[8] Hof and co-workers have recently reported that *tetraanionic* calixarenes would, in aqueous environments, dimerize (K_d ~ 1 mM) despite holding equivalent charges.[9] Moreover, ionic salts (NaCl, $MgCl_2$, etc.) increased the stability of such complexes by screening negative sites[10] and assisting the hydrophobic effect.[11] In the course of studying nesting complexes,[12] we found that cup-shaped and trianionic $[\mathbf{1}_{syn}]^{3-}$ (Figure 1A) would only trap positively charged C_3 symmetric guests. The complexations were driven by hydrophobic effect[13] and supported by salt-bridge contacts.[14] Moreover, trianionic $[\mathbf{1}_{syn}]^{3-}$ showed no tendency to self-associate in water despite its sizeable and nonpolar surface.[15] Considering the propensity of structurally related and dianionic molecular tweezers to dimerize (K_d ~ 10 μM),[16] we wondered if chair-shaped and trianionic $[\mathbf{1}_{anti}]^{3-}$ (Figure 1B) would assemble in aqueous media and give hexaanionic or even more charged aggregates?[17] In fact, Monte Carlo conformational sampling (MC/MM: OPLS3, Maestro) of $[\mathbf{1}_{anti}]^{3-}$ suggested two modes by which it could

Department of Chemistry & Biochemistry, The Ohio State University
100 West 18th Avenue, 43210 Columbus, Ohio USA. E-mail: badjic.1@osu.edu
† Electronic Supplementary Information (ESI) available: [Experimental details, additional spectra and computations]. See DOI: 10.1039/x0xx00000x

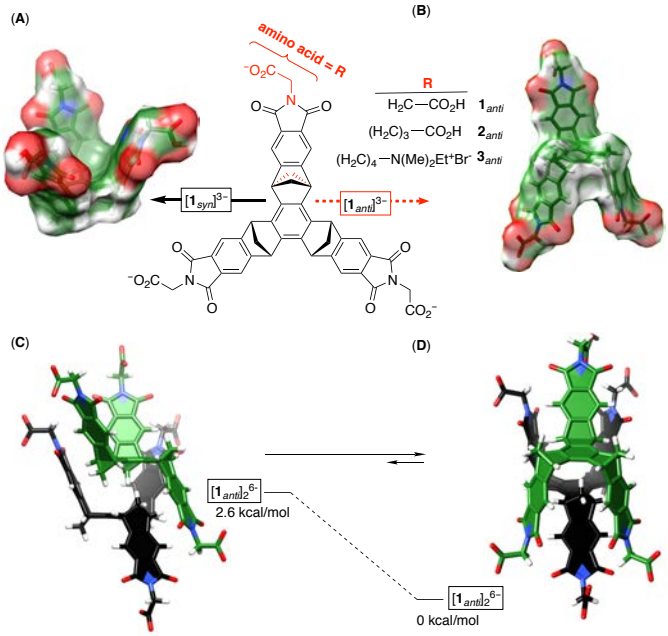

Figure 1. Chemical structures of $[\mathbf{1}_{syn}]^{3-}$ (black) and $[\mathbf{1}–\mathbf{3}_{anti}]^{3-}$ (red) with van der Waals surfaces of cup-shaped $[\mathbf{1}_{syn}]^{3-}$ (A) and chair-shaped $[\mathbf{1}_{anti}]^{3-}$ (B). Energy-minimized structures (MC/MM, OPLS3) of parallel $[\mathbf{1}_{anti}]_2^{6-}$ (C) and antiparallel $[\mathbf{1}_{anti}]_2^{6-}$ (D) homodimers with computed steric energies in implicit water solvent.

stack: (a) parallel, giving less stable and twisted $[\mathbf{1}_{anti}]_2^{6-}$ (Figure 1C) and (b) antiparallel, giving more stable $[\mathbf{1}_{anti}]_2^{6-}$ (Figure 1D); note that parallel $[\mathbf{1}_{anti}]_2^{3-}$ may as well grow into a helical supramolecular polymer. In line with the theory, we decided to prepare molecular chairs $\mathbf{1}_{anti}$–$\mathbf{3}_{anti}$ (Figure 1B) carrying positively or negatively charged groups, and then probe their assembly in water, with and without kosmotropic (NaCl) and chaotropic ($NaClO_4$) anions.[18]

Compounds $\mathbf{1}_{anti}$–$\mathbf{3}_{anti}$ (Figure 1B) were obtained by condensation reactions (Scheme S1).[19] A slow evaporation of acetonitrile solution of $\mathbf{1}_{anti}$ gave single crystals, which after X-ray diffraction analysis revealed molecular chairs packed in a parallel mode along arbitrary crystallographic axis *a* (Figure 2) thereby forming C–H---O intermolecular contacts.[20] Along the axis *b*, however, the adjacent chairs are "stitched" by carboxylate groups. That is to say, one carboxylate from the lone phthalimide bisects the gap between two neighbouring

phthalimides whereby it is held by four C–H---O hydrogen bonds[20] (D = 3.229–3.538 Å; 1–4 in Figure 2) and two n–to–π*[21] or dipolar interactions[22] (d = 3.102 and 3.560 Å; Figure 2); for n–to–π* like contacts, O---C=O angles Θ are 84 and 76º and therefore below the expected Θ = 109 ± 10º.[21] ^{1}H NMR spectrum of $\mathbf{1}_{anti}$ in DMSO showed a single set of resonances corresponding to, on average, C_s symmetric molecule (Figure 3). Using ^{1}H–^{1}H NOESY correlations (Figure

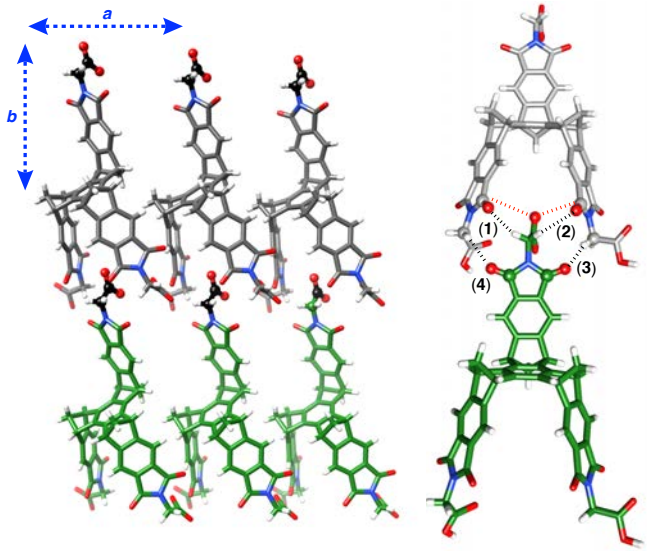

Figure 2. X-ray structure of $\mathbf{1}_{anti}$ along arbitrarily assigned crystallographic axes *a* and *b*. (Right) Fragments of interdigitating chairs forming four C–H---O hydrogen bonds (**1**-**4**, black dashed lines) and two n-to-π* like contacts (red dashed lines).

S11), we assigned the signals from $\mathbf{1}_{anti}$ with diastereotopic $\mathbf{H}_{A/A1}$ (δ = 4.2 ppm) appearing as a singlet. The two nuclei are, perhaps, faraway from the *tris*-bicyclic hub to turn chemically equivalent by averaging into a singlet (*vide infra*). After 50-fold dilution of 5.0 mM of $\mathbf{1}_{anti}$ in CD_3SOCD_3, there were rather small ^{1}H NMR spectroscopic changes to indicate the absence of aggregation (Figure S12). After we placed $\mathbf{1}_{anti}$ into 0.1 M phosphate buffer (NaH_2PO_4/Na_2HPO_4) at pH = 7.2, however, there followed its complete dissolution and the formation of trianionic $[\mathbf{1}_{anti}]^{3-}$ (pK_a<5) with ^{1}H NMR spectrum (5.9 mM, Figure 4A) showing a set of well-resolved resonances; ^{1}H–^{1}H NOESY cross-correlations (Figure S13) were sufficient to assign all of the signals from $[\mathbf{1}_{anti}]^{3-}$. To probe self-association of $[\mathbf{1}_{anti}]^{3-}$ in water, we recorded its ^{1}H NMR spectra at various concentrations (Figure 4A). To our delight, a gradual dilution of 5.9 mM solution of $[\mathbf{1}_{anti}]^{3-}$ caused a steady change in the chemical shift of its resonances with the majority of nuclei becoming magnetically deshielded (Figure 4B). The hyperbolic dependence of chemical shifts as a function of concentration suggested self-association while diamagnetic anisotropy effects indicated that chairs, holding aromatics, reside at a close distance. To probe if dimerization of $[\mathbf{1}_{anti}]^{3-}$ took place, the complexation data were fit to two-state dimerization model[23] (the Occam's razor principle) using the least-square regression analysis (Figure 4B; see also Figure S15). A random distribution of residuals together with the satisfactory fit of the experimental data (R^2 = 0.99) was in line with $[\mathbf{1}_{anti}]^{3-}$ forming homodimers $[\mathbf{1}_{anti}]_2^{6-}$ (K_a = 410 ± 10 M^{-1}, Table 1). After we completed the measurement in 25 mM (instead of 0.1 M) phosphate buffer (Figure S16), $[\mathbf{1}_{anti}]_2^{6-}$ was found to possess a lower stability (K_a = 152 ± 60 M^{-1}, Table 1). Allegedly, sodium cations from the buffer screen anionic charges[8] within $[\mathbf{1}_{anti}]_2^{6-}$

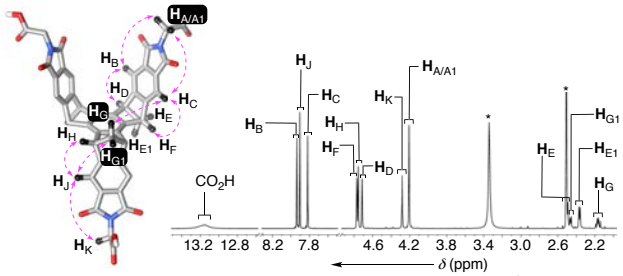

Figure 3. Energy-minimized (MMFF, Spartan) structure of $\mathbf{1}_{anti}$ and its ^{1}H NMR spectrum (600 MHz, 298 K) in CD_3SOCD_3. Pink dotted lines describe important NOE's (Figure S11).

to improve its stability while phosphate anions act as kosmotropes in assisting the hydrophobic effect ("salting out" anions in the Hofmeister series).[2] To further examine the formation of $[\mathbf{1}_{anti}]_2^{6-}$, we used ^{1}H NMR diffusion spectroscopy and measured apparent diffusion coefficients D_{app} of $[\mathbf{1}_{anti}]^{3-}$ at different concentrations (Figure S17).[24] With the exchange of proton resonances of $[\mathbf{1}_{anti}]^{3-}$ and, presumably, $[\mathbf{1}_{anti}]_2^{6-}$ being fast on ^{1}H NMR time scale, the measured D_{app} is a weighted average of diffusion coefficients of monomeric (D_m) and dimeric (D_d) molecules: $D_{app} = n_m \cdot D_m + n_d \cdot D_d$, with n_m and n_d depicting molar fractions of $[\mathbf{1}_{anti}]^{3-}$ and $[\mathbf{1}_{anti}]_2^{6-}$.[25] Since $n_m + n_d = 1$, one can derive $D_{app} = n_m (D_m - D_d) + D_d$ from which it follows that D_{app} is linearly proportional to n_m. From stability constant K_a = 152 M^{-1} (Table 1), we calculated the corresponding molar fractions n_m of monomeric $[\mathbf{1}_{anti}]^{3-}$ at its different initial concentrations, and after plotting the data indeed found a linear relationship between D_{app} and n_m (Figure 4C). The linear least-square analysis gave $D_m = 3.7 \cdot 10^{-10}$ m^2/s and $D_d = 2.0 \cdot 10^{-10}$ m^2/s, which from the Einstein-Stock equation[24] gave hydrodynamic radii for monomeric $[\mathbf{1}_{anti}]^{3-}$ (6.5 Å) and dimeric $[\mathbf{1}_{anti}]_2^{6-}$ species (12.1 Å); note that r_d/r_m = 1.85. In this regard, the results of DLS measurements of $[\mathbf{1}_{anti}]^{3-}$ (Figure S28) indicated the absence of oligomers with the observed distribution of hydrodynamic diameters (D_H) from 0.6 to 2.7 nm. What is the geometry of the assembled molecular chairs? As stated earlier, two potential scenarios include parallel (Figure 1C) and antiparallel (Figure 1D) stacks. In this regard, the formation of $[\mathbf{1}_{anti}]_2^{6-}$ caused a disproportionally large magnetic perturbation of bridge $\mathbf{H}_G/\mathbf{H}_{G1}$ ($\Delta\delta$ = –1.2 ppm, Figure 4B) and bridgehead $\mathbf{H}_H$ ($\Delta\delta$ = –0.6 ppm, Figure 4B) nuclei to imply that this part of one chair resides against the aromatics from another chair. With both assembly modes in Figure 1C/D having bridge $\mathbf{H}_G/\mathbf{H}_{G1}$ protons situated against aromatic rings, we sought additional evidence to elucidate the complexation geometry. Accordingly, ^{1}H–^{1}H NOESY examinations of $[\mathbf{1}_{anti}]_2^{6-}$ (Figures 4D and S13/14) showed cross-correlations between $\mathbf{H}_{G1}/\mathbf{H}_C$ and $\mathbf{H}_A/\mathbf{H}_J$ protons. These nuclei are in monomeric $[\mathbf{1}_{anti}]^{3-}$ (Figure 4B) as well as in parallel dimer $[\mathbf{1}_{anti}]_2^{6-}$ separated by >6.1 Å. For antiparallel and C_{2h} symmetric $[\mathbf{1}_{anti}]_2^{6-}$ (Figure 4D), however, $\mathbf{H}_{G1}/\mathbf{H}_C$ and $\mathbf{H}_A/\mathbf{H}_J$ are 4.3 and 2.5 Å apart and thus close enough for the dipolar

spin-spin coupling! Moreover, from the energy-minimized structure of antiparallel $[\mathbf{1}_{anti}]_2$ (DFT/B3LYP:6-31G*, Figure 4D), we could distinguish several noncovalent contacts holding the complex together. First, bridge $\mathbf{H}_{G/G1}$ protons from one chair fit well within the "aromatic saddle" of another chair (Figure 4D), with $\mathbf{H}_{G1}$ poised to form three whereas $\mathbf{H}_G$ only one C–H---π contacts (4.1–4.5 Å carbon-to-π centroid distances).[25-26] With $\mathbf{H}_{G1}$ being more magnetically shielded than $\mathbf{H}_G$ (Figure 4B), we concluded that the computational results were in register with the experimental findings. Second, C–$\mathbf{H}_A$ group at the rim of each molecular chair is within C–H---O hydrogen bonding range (<4 Å, Figure 4D)[20] of the carbonyl imide oxygen from another chair. These hydrogen bonds could (a) bias the conformation of the glycine moiety and (b) cause a magnetic deshielding of $\mathbf{H}_A$ but not $\mathbf{H}_{A1}$ protons. Indeed, increase in the population of $[\mathbf{1}_{anti}]_2^{6-}$ dimeric state (Figure 4A) caused the conversion of singlet corresponding to $\mathbf{H}_{A/A1}$ into AB quartet with the resonance from $\mathbf{H}_A$ but not $\mathbf{H}_{A1}$ shifting downfield.

At first glance, the formation of antiparallel $[\mathbf{1}_{anti}]_2^{6-}$ in solution did not take place in the solid state (Figure 2). In this regard, single crystals of $\mathbf{1}_{anti}$ (not $[\mathbf{1}_{anti}]^{3-}$) were grown from acetonitrile (not water) with the packing forces favouring the observed arrangement of neutral (not trianionic) chairs.

As described earlier, a greater quantity of sodium cations/phosphate anions enhanced the stability of hexa-anionic $[\mathbf{1}_{anti}]_2^{6-}$ (K_a = from 152 to 410 M^{-1}, Table 1). Likewise, raising the ionic strength with NaCl additionally improved the homophilicity of $[\mathbf{1}_{anti}]^{3-}$ (K_a = from 410 to 570 M^{-1}, Table 1; Figure S18). We reason that sodium cations along with strongly solvated kosmotropes, phosphate and chlorides, ought to be shielding[8] the charges of hexaanionic $[\mathbf{1}_{anti}]_2^{6-}$ and concurrently assist the hydrophobic association.[18a] On the other hand, weakly solvated chaotropes (i.e. ClO_4^-) are known to interact with aromatic surfaces and thereby weaken hydrophobically driven complexations.[27] The addition of $NaClO_4$ to a solution of $[\mathbf{1}_{anti}]_2^{6-}$ improved its stability (K_a = from 410 to 458 M^{-1}, Table 1; Figure S19) albeit to a lesser degree than NaCl. To a first approximation, sodium cations screen the anionic sites in $[\mathbf{1}_{anti}]_2^{6-}$ with the adverse solvation of aromatic surfaces by perchlorates assuming the secondary role. To further investigate the stacking of molecular chairs, we examined the behaviour of trianionic $[\mathbf{2}_{anti}]^{3-}$ and tricationic $[\mathbf{3}_{anti}]^{3+}$ (Figure 5A/B). These molecules have their point charges situated at the tip of "flexible" aliphatic chains, away from the aromatic scaffold. On the basis of ^{1}H NMR results (Figures S18–S19), both $[\mathbf{2}_{anti}]^{3-}$ and $[\mathbf{3}_{anti}]^{3+}$ assembled into antiparallel homodimers. Thermodynamic stabilities of $[\mathbf{2}_{anti}]_2^{6-}$ and $[\mathbf{3}_{anti}]_2^{6+}$ were, however, an order of magnitude greater than of $[\mathbf{1}_{anti}]_2^{6-}$ (Table 1). Apparently, placing anionic or cationic sites onto a "flexible" chain and at a greater distance minimized the adverse intermolecular contacts to facilitate the stacking. The formation of heterodimer $[\mathbf{2}_{anti}]^{3-}\subset[\mathbf{3}_{anti}]^{3+}$ (Figure 5C) was corroborated with ^{1}H NMR spectroscopy (Figures S22–S24) while ESI mass spectrometry provided additional evidence in support of 1:1 stoichiometry (Figure S25). The stability or $[\mathbf{2}_{anti}\subset\mathbf{3}_{anti}]$ was found to be $K_a = 3.3 \cdot 10^4$ M^{-1} (Table 1) and an order of magnitude greater than in the case of the corresponding homodimers. Importantly, an increase in the

Table 1. Thermodynamic stabilities K_a (M^{-1}) of homo- and heterodimers were, in water at pH = 7.2 and 298 K, determined by non-linear least square analysis of binding isotherms (^{1}H NMR spectroscopy); PB stands for phosphate buffer. Each measurement was repeated twice, with the reported value representing arithmetic mean and the error margin corresponding to the standard deviation.

K_a (M^{-1})	$[1_{anti}]_2^{6-}$	$[2_{anti}]_2^{6-}$	$[3_{anti}]_2^{6+}$	$[2_{anti}\subset 3_{anti}]$
25 mM PB	152 ± 60	1704 ± 42	2087 ± 13	$3.3 \pm 0.2 \cdot 10^4$
0.1 M PB	410 ± 10	–	–	–
0.1 M PB/NaCl	570 ± 62	–	–	$1.3 \pm 0.2 \cdot 10^4$
0.1 M PB/$NaClO_4$	458 ± 11	–	–	–

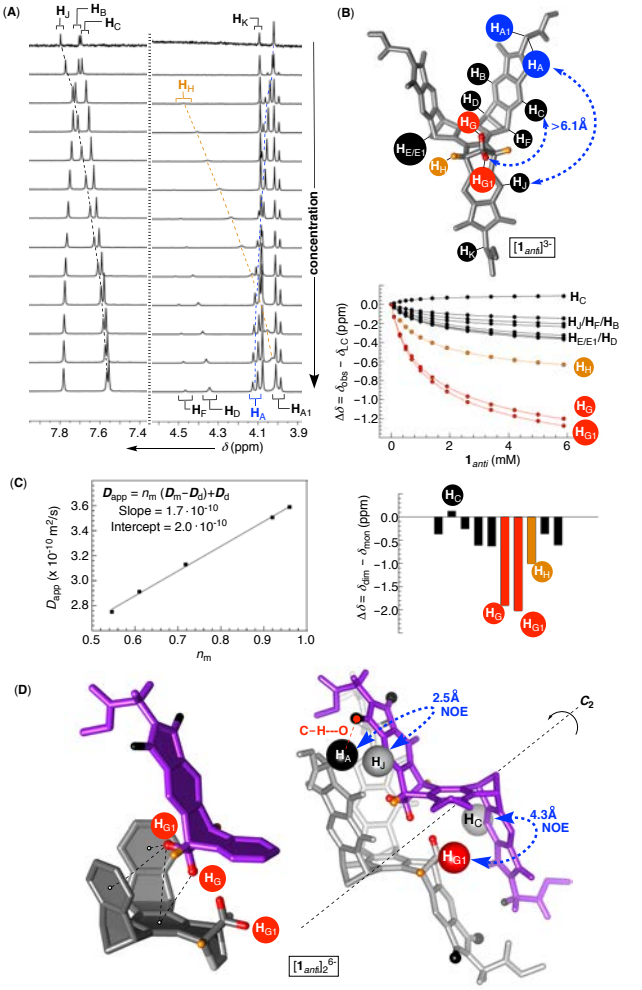

Figure 4. (A) Partial ^{1}H NMR spectra (600 MHz, 298 K) of 5.9 mM to 0.5 μM aqueous solution of $[\mathbf{1}_{anti}]^{3-}$ (bottom to top; 25 mM phosphate buffer at pH = 7.2). (B) ^{1}H NMR change in the chemical shifts $\Delta\delta$ (ppm) of protons from $[\mathbf{1}_{anti}]^{3-}$ upon diluting its 5.9 mM solution (A). The data were fit to two-state dimerization model (SigmaPlot) using least-square regression analysis to give K_a = 152 ± 60 M^{-1}. Note that for the top plot, $\Delta\delta$ depicts a difference between the observed chemical shift δ_{obs} of the chair's protons and corresponding chemical shifts δ_{LC} at its lowest concentration. In the bottom graph, $\Delta\delta$ describes a difference between chemical shifts of protons within dimeric $[\mathbf{1}_{anti}]_2^{6-}$ and monomeric $[\mathbf{1}_{anti}]^{3-}$ as obtained from the fitting. (C) A change in the apparent diffusion coefficient D_{app} of $[\mathbf{1}_{anti}]^{3-}$ (25 mM phosphate buffer at pH = 7.2, 298 K) as a function of its concentration was fit to linear equation $D_{app} = n_m (D_m - D_d) + D_d$. (D) Fragments of energy-minimized (DFT/B3LYP:6-31G*, Spartan) structure of $[\mathbf{1}_{anti}]_2$ (methyl ester derivative) showing noncovalent intermolecular contacts, NOEs and computed distances.

solution's ionic strength weakened the association (K_a = 1.3 · 10^4 M^{-1}, Table 1) as the attractive host-guest ionic contacts within zwitterionic [$\mathbf{2}_{anti}$⊂$\mathbf{3}_{anti}$] (i.e. salt bridges in Figure 5C) became shielded.[8] As a proof of concept, the dimerization of [$\mathbf{8}_{anti}$]$^{3-}$ holding three Gly–Gly–Gly peptides occurred in the expected antiparallel fashion to give [$\mathbf{8}_{anti}$]$_2^{6-}$ (Figure 5D). In particular, the stability of multivalent [$\mathbf{8}_{anti}$]$_2^{6-}$ increased from K_a = 510 to 1.3 · 10^3 M^{-1} with the addition of sodium phosphate and chloride salts, (Figure S26–S27) to assist with (a) a shielding of negative charges from six peptide chains and (b) the hydrophobic association.

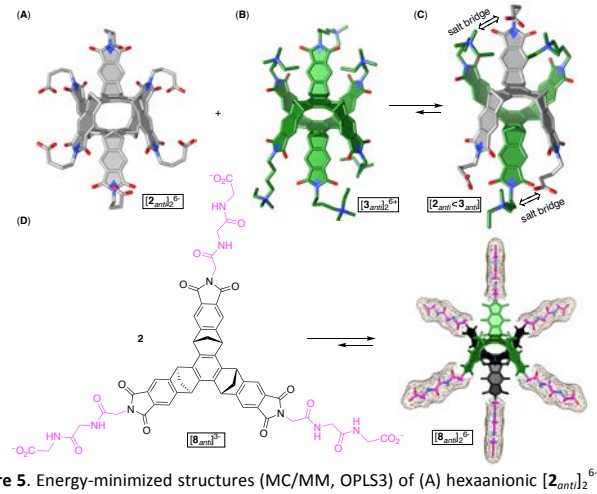

Figure 5. Energy-minimized structures (MC/MM, OPLS3) of (A) hexaanionic [$\mathbf{2}_{anti}$]$_2^{6-}$, (B) hexacationic [$\mathbf{3}_{anti}$]$_2^{6+}$ and (C) zwitterionic [$\mathbf{2}_{anti}$⊂$\mathbf{3}_{anti}$] forming salt bridges in implicit water solvent. For each calculation, antiparallel dimers were found to populate over 90% of the equilibrium. (D) Chemical structure of *tris*-Gly-Gly-Gly [$\mathbf{8}_{anti}$]$^{3-}$ and its energy-minimized (MMFF, Spartan) [$\mathbf{8}_{anti}$]$_2^{6-}$.

In conclusion, molecular chairs carrying charged and functional groups at their periphery stack in antiparallel manner to form homo- and heterodimers. The stability of homodimeric assemblies increases in the presence of kosmotropic and chaotropic salts suggesting a potential utility of these systems in biological media.[9] As stacked molecular chairs display amino acids or peptides in unique multivalent fashion,[28] here described finding should help designing functional nanostructures[29] and therapeutics,[30] about which we aim to report in the future.

Acknowledgements

This work was financially supported with funds obtained from the National Science Foundation under CHE-1606404.

Notes and references

(1) Aida, T.; Meijer, E. W.; Stupp, S. I. *Science* **2012**, *335*, 813.
(2) Cremer, P. S.; Flood, A. H.; Gibb, B. C.; Mobley, D. L. *Nat. Chem.* **2018**, *10*, 8.
(3) Biedermann, F.; Nau, W. M.; Schneider, H.-J. *Angew. Chem., Int. Ed.* **2014**, *53*, 11158.
(4) aOshovsky, G. V.; Reinhoudt, D. N.; Verboom, W. *Angew. Chem., Int. Ed.* **2007**, *46*, 2366; bBiedermann, F.; Schneider, H.-J. *Chem. Rev.* **2016**, *116*, 5216.
(5) Israelachvili, J. N. *Intermolecular and Surface Forces*, 2011.
(6) (a) Shimizu, T.; Masuda, M.; Minamikawa, H. *Chem. Rev.* **2005**, *105*, 1401; (b) Okesola, B. O.; Smith, D. K. *Chem. Soc. Rev.* **2016**, *45*, 4226; (c) Rieth, S.; Baddeley, C.; Badjic, J. D. *Soft Matter* **2007**, *3*, 137; (d) Hendricks, M. P.; Sato, K.; Palmer, L. C.; Stupp, S. I. *Acc. Chem. Res.* **2017**, *50*, 2440; (e) Stupp, S. I.; Palmer, L. C. *Chem. Mater.* **2014**, *26*, 507; (f) Border, S. E.; Pavlovic, R. Z.; Zhiquan, L.; Gunther, M. J.; Wang, H.; Cui, H.; Badjic, J. D. *Chem. Eur. J.* **2019**, *25*, 273.
(7) (a) Fiammengo, R.; Timmerman, P.; de Jong, F.; Reinhoudt, D. N. *Chem. Commun.* **2000**, 2313; (b) Corbellini, F.; Di Costanzo, L.; Crego-Calama, M.; Geremia, S.; Reinhoudt, D. N. *J. Am. Chem. Soc.* **2003**, *125*, 9946; (c) Corbellini, F.; Fiammengo, R.; Timmerman, P.; Crego-Calama, M.; Versluis, K.; Heck, A. J. R.; Luyten, I.; Reinhoudt, D. N. *J. Am. Chem. Soc.* **2002**, *124*, 6569; dSchneider, H. J.; Schiestel, T.; Zimmermann, P. *J. Am. Chem. Soc.* **1992**, *114*, 7698; (e) Zadmard, R.; Junkers, M.; Schrader, T.; Grawe, T.; Kraft, A. *J. Org. Chem.* **2003**, *68*, 6511; (f) Kim, S. K.; Sessler, J. L. *Acc. Chem. Res.* **2014**, *47*, 2525; (g) Metzger, A.; Lynch, V. M.; Anslyn, E. V. *Angew. Chem., Int. Ed. Engl.* **1997**, *36*, 862; (h) Yu, G.; Zhou, J.; Shen, J.; Tang, G.; Huang, F. *Chem. Sci.* **2016**, *7*, 4073.
(8) Schneider, H.-J. *Angew. Chem., Int. Ed.* **2009**, *48*, 3924.
(9) Garnett, G. A. E.; Daze, K. D.; Pena Diaz, J. A.; Fagen, N.; Shaurya, A.; Ma, M. C. F.; Collins, M. S.; Johnson, D. W.; Zakharov, L. N.; Hof, F. *Chem. Commun.* **2016**, *52*, 2768.
(10) Hossain, M. A.; Schneider, H.-J. *Chem. Eur. J.* **1999**, *5*, 1284.
(11) Gibb, C. L. D.; Oertling, E. E.; Velaga, S.; Gibb, B. C. *J. Phys. Chem. B* **2015**, *119*, 5624.
(12) Zhiquan, L.; Polen, S.; Hadad, C. M.; RajanBabu, T. V.; Badjic, J. D. *J. Am. Chem. Soc.* **2016**, *138*, 8253.
(13) Gibb, B. C. *Chemosensors* **2011**, 3.
(14) Zhiquan, L.; Polen, S. M.; Hadad, C. M.; RajanBabu, T. V.; Badjic, J. D. *Org. Lett.* **2017**, *19*, 4932.
(15) Border, S. E.; Pavlovic, R. Z.; Zhiquan, L.; Badjic, J. D. *J. Am. Chem. Soc.* **2017**, *139*, 18496.
(16) Branchi, B.; Ceroni, P.; Balzani, V.; Cartagena, M. C.; Klaerner, F.-G.; Schrader, T.; Vogtle, F. *New J. Chem.* **2009**, *33*, 397.
(17) (a) Nguyen, M. T.; Ferris, D. P.; Pezzato, C.; Wang, Y.; Stoddart, J. F. *Chem* **2018**, *4*, 2329; (b) Fatila, E. M.; Twum, E. B.; Sengupta, A.; Pink, M.; Karty, J. A.; Raghavachari, K.; Flood, A. H. *Angew. Chem., Int. Ed.* **2016**, *55*, 14057.
(18) (a) Zhang, Y.; Cremer, P. S. *Curr. Opin. Chem. Biol.* **2006**, *10*, 658; (b) Gibb, B. C. *Isr. J. Chem.* **2011**, *51*, 798; (c) Sullivan, M. R.; Yao, W.; Tang, D.; Ashbaugh, H. S.; Gibb, B. C. *J. Phys. Chem. B* **2018**, *122*, 1702.
(19) Chen, S.; Ruan, Y.; Brown, J. D.; Gallucci, J.; Maslak, V.; Hadad, C. M.; Badjic, J. D. *J. Am. Chem. Soc.* **2013**, *135*, 14964.
(20) Desiraju, G. R. *Acc. Chem. Res.* **1996**, *29*, 441.
(21) Newberry, R. W.; Raines, R. T. *Acc. Chem. Res.* **2017**, *50*, 1838.
(22) Allen, F. H.; Baalham, C. A.; Lommerse, J. P. M.; Raithby, P. R. *Acta Crystallogr., Sect. B Struct. Sci.* **1998**, *B54*, 320.
(23) Chen, J. S.; Shirts, R. B. *J. Phys. Chem.* **1985**, *89*, 1643.
(24) Cohen, Y.; Avram, L.; Frish, L. *Angew. Chem., Int. Ed.* **2005**, *44*, 520.
(25) Ruan, Y.; Peterson, P. W.; Hadad, C. M.; Badjic, J. D. *Chem. Commun.* **2014**, *50*, 9086.
(26) Nishio, M.; Umezawa, Y.; Fantini, J.; Weiss, M. S.; Chakrabarti, P. *Phys. Chem. Chem. Phys.* **2014**, *16*, 12648.
(27) Gibb, C. L. D.; Gibb, B. C. *J. Am. Chem. Soc.* **2011**, *133*, 7344.
(28) Liu, S. P.; Zhou, L.; Lakshminarayanan, R.; Beuerman, R. W. *Int. J. Pept. Res. Ther.* **2010**, *16*, 199.
(29) (a) Sato, K.; Hendricks, M. P.; Palmer, L. C.; Stupp, S. I. *Chem. Soc. Rev.* **2018**, *47*, 7539; (b) Wang, Z.; An, G.; Zhu, Y.; Liu, X.; Chen, Y.; Wu, H.; Wang, Y.; Shi, X.; Mao, C. *Mater. Horiz.* **2019**, Ahead of Print; (c) Garcia, A. M.; Kurbasic, M.; Kralj, S.; Melchionna, M.; Marchesan, S. *Chem. Commun.* **2017**, *53*, 8110.
(30) (a) Henninot, A.; Collins, J. C.; Nuss, J. M. *J. Med. Chem.* **2018**, *61*, 1382; (b) Lau, J. L.; Dunn, M. K. *Bioorg. Med. Chem.* **2018**, *26*, 2700.

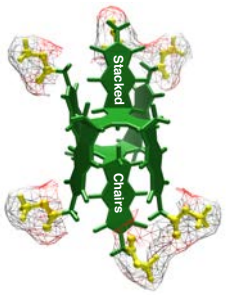

Molecular chairs, carrying three amino acids or peptides, stack in antiparallel fashion to give hexavalent assemblies for bottom-up construction of novel soft materials and therapeutics.